

Article

Examining the Effects of an Anti-Salmonella Bacteriophage Preparation, BAFASAL[®], on Ex-Vivo Human Gut Microbiome Composition and Function Using a Multi-Omics Approach

Janice Mayne ¹, Xu Zhang ¹, James Butcher ¹, Krystal Walker ¹, Zhibin Ning ¹, Ewelina Wójcik ², Jarosław Dastych ^{2,*}, Alain Stintzi ^{1,3} and Daniel Figeys ^{1,3,*}

¹ Department of Biochemistry, Microbiology and Immunology, Faculty of Medicine, University of Ottawa, Ottawa, ON K1H-8M5, Canada; jmayn2@uottawa.ca (J.M.); xzhan7@uottawa.ca (X.Z.); jbutcher@uottawa.ca (J.B.); kwalker2@uottawa.ca (K.W.); zning@uottawa.ca (Z.N.); astintzi@uottawa.ca (A.S.)
² Proteon Pharmaceuticals SA, Tylna 3a, 90-364 Łódź, Poland; ewojcik@proteonpharma.com
³ MedBiome Inc., Ottawa, ON K1H-8M5, Canada
* Correspondence: jdastych@proteonpharma.com (J.D.); dfigeys@uottawa.ca (D.F.)



Citation: Mayne, J.; Zhang, X.; Butcher, J.; Walker, K.; Ning, Z.; Wójcik, E.; Dastych, J.; Stintzi, A.; Figeys, D. Examining the Effects of an Anti-Salmonella Bacteriophage Preparation, BAFASAL[®], on Ex-Vivo Human Gut Microbiome Composition and Function Using a Multi-Omics Approach. *Viruses* **2021**, *13*, 1734. <https://doi.org/10.3390/v13091734>

Academic Editors:
Zuzanna Drulis-Kawa and
Daria Augustyniak

Received: 22 July 2021
Accepted: 23 August 2021
Published: 31 August 2021

Publisher's Note: MDPI stays neutral with regard to jurisdictional claims in published maps and institutional affiliations.



Copyright: © 2021 by the authors. Licensee MDPI, Basel, Switzerland. This article is an open access article distributed under the terms and conditions of the Creative Commons Attribution (CC BY) license (<https://creativecommons.org/licenses/by/4.0/>).

Abstract: *Salmonella* infections (salmonellosis) pose serious health risks to humans, usually via food-chain contamination. This foodborne pathogen causes major food losses and human illnesses, with significant economic impacts. Overuse of antibiotics in the food industry has led to multidrug-resistant strains of bacteria, and governments are now restricting their use, leading the food industry to search for alternatives to secure food chains. Bacteriophages, viruses that infect and kill bacteria, are currently being investigated and used as replacement treatments and prophylactics due to their specificity and efficacy. They are generally regarded as safe alternatives to antibiotics, as they are natural components of the ecosystem. However, when specifically used in the industry, they can also make their way into humans through our food chain or exposure, as is the case for antibiotics. In particular, agricultural workers could be repeatedly exposed to bacteriophages supplemented to animal feeds. To our knowledge, no studies have investigated the effects of such exposure to bacteriophages on the human gut microbiome. In this study, we used a novel in-vitro assay called RapidAIM to investigate the effect of a bacteriophage mixture, BAFASAL[®], used in poultry farming on five individual human gut microbiomes. Multi-omics analyses, including 16S rRNA gene sequencing and metaproteomic, revealed that ex-vivo human gut microbiota composition and function were unaffected by BAFASAL[®] treatment, providing an additional measure for its safety. Due to the critical role of the gut microbiome in human health and the known role of bacteriophages in regulation of microbiome composition and function, we suggest assaying the impact of bacteriophage-cocktails on the human gut microbiome as a part of their safety assessment.

Keywords: bacteriophage; microbiome; *Salmonella*; metaproteomics; 16S rRNA gene sequencing; BAFASAL[®]

1. Introduction

As the world population increases, so does food demand. Plant and animal diseases can seriously impact food supplies and food safety, resulting in food shortages and causing significant economic impacts. Zoonotic diseases present clear public health risks; in the USA, tens of thousands get sick each year, with six out of 10 infectious diseases having a zoonotic origin [1]. Strikingly, the World Health Organization (WHO) estimates that consumption of contaminated food sickens 600 million people (or 10% of the world population), and results in 420,000 deaths [2].

Historically, most zoonotic diseases have been treated with antibiotics, with 73% of all antibiotics in the world now used in animal production [3]. The wide-spread use of antibiotics in the food industry was spurred on not only by increased food safety but by data

showing increased meat production in animals receiving broad-spectrum antibiotics [4]. The appearance of multidrug-resistant bacteria in our food chain is an unintended consequence from decades of over-using broad-spectrum antibiotics. In addition, humans are exposed to these excess antibiotics through several means: these antibiotics can be present in the animal products we consume and can be simply discarded into the environment, with up to 90% of antibiotics excreted in their active forms from treated animals [5]. The rise of multidrug-resistant bacteria has become such a global concern that by 2022, the European Union (EU) will ban the prophylactic use of clinically relevant antibiotics in food production, with the exemption of veterinary prescriptions [6], and other countries are following suit. Without such interventions, antimicrobial resistance (AMR) will result in an estimated 10 million deaths by 2050 [5].

Nevertheless, the issue of food safety and the prevention of zoonotic diseases remain. Bacteriophage therapy is an alternative garnering increased interest by scientists and food agencies around the world. Discovered by Félix d’Hérelle and Frederick Twort in the early 1900s, bacteriophages have been investigated for their therapeutic potential to treat pathogenic bacteria in humans, animals, and agriculture, especially in light of AMR [7]. Bacteriophages, or phages, are ubiquitous and abundant in nature, with numbers estimated above 10^{31} [8]. Indeed, phages outnumber their bacterial hosts by a factor of 10 times and regulate the bacterial populations they target by triggering bacterial lysis. Their ability to act directly on specific bacteria—via their recognition of unique receptor proteins—allows researchers to develop targeted therapies to fight against identifiable bacterial pathogens in our food chain and reduce the spread of foodborne illnesses in humans.

Bacteriophage therapy in the food industry has proven successful: phages have been approved for use in food decontamination [9], as dietary supplements [10], and as environmental prophylaxis [11]. Importantly, no adverse effects were noted in trials, as phages did not interact with eukaryotic cells and targeted only bacteria [11]. One of the most common foodborne illnesses, Salmonellosis, is caused by the bacterium *Salmonella*. *Salmonella* easily transfers from its primary hosts (commonly laying hens, pigs, turkeys, and broilers) to humans and is a common target for bacteriophage cocktails [12]. *Salmonella* is a genus of the family *Enterobacteriaceae* and contains two species: *S. enterica* and *S. bongori* [13]. Salmonellosis causes fever, sepsis, infection of tissues, and inflammation of the gastrointestinal tract. In America alone, *Salmonella* genera cause 1.35×10^6 infections, resulting in 26,000 hospitalizations and 420 deaths each year [1]. In the EU, salmonellosis is the most common foodborne disease and *S. enterica* the most frequently reported pathogen. In 2020, a study profiled the effectiveness of an anti-*Salmonella* bacteriophage cocktail, BASFASAL, to prevent contamination of dried and liquid poultry feed in vitro and to reduce numbers of *Salmonella* in intestines of birds challenged with *Salmonella* in vivo [12].

The human gut microbiome, consisting of bacteria, viruses, and fungi, plays a critical role in health, as evidenced by perturbations in the gut microbiome composition and/or function that associated with a variety of diseases, including inflammatory bowel diseases (IBD) [14], cardiovascular disease [15], Parkinson’s and Alzheimer’s diseases [16,17], anxiety, and depression [18]. Bacteriophages are a normal part of the human microbiota and also outnumber bacteria in our gut by at least ten-fold. Most are temperate phages, and so induction of these prophages under various conditions could disturb microbiota balance [19]. Although bacteriophages are generally recognized as safe (GRAS) when used for pathogen control in food processing, including ready to eat foods and poultry, bacteriophages could interact with niche gut microbiota [19]. Effects could range from no effect to direct lysis and dysbiosis of commensal bacterial to indirect interactions of bacteriophage with commensal bacteria or prophages, triggering lysis [19].

We have developed an in-vitro gut microbiome culturing system (MiPro) coupled to a downstream bioinformatics toolbox collectively called RapidAIM (or rapid assay of an individual microbiome) that measures compositional and functional changes in the gut microbiome in response to dietary and therapeutic interventions [20,21]. RapidAIM can measure the impact of products on the microbiota and can be used to stratify people

in clinical studies. We previously used this assay to show the effects of antibiotics and other drugs on the gut microbiome [20]. In this study, we used RapidAIM to investigate further the effects of BAFASAL[®]: specifically, whether BAFASAL[®] phage introduction to the human gut microbiome affects its composition and function. We treated five individual adult-derived gut microbiomes with active and inactive mixtures of BAFASAL[®]. We used both 16S rRNA gene sequencing and metaproteomic analyses to study changes in bacterial composition and function. This study, the first of its kind, has important implications for how we measure food safety and maintain the safety of workers in the food-processing industry exposed to these preparations.

2. Materials and Methods

2.1. BAFASAL[®] Production

Liquid BAFASAL[®] preparation was produced according to Wójcik et al. [12]. Briefly, bacteriophages included in BAFASAL[®] (BAF) were amplified separately in culture, reaching a titer of about 1×10^9 PFU/mL. Phage-containing culture fluid was separated from bacterial debris by filtration, and final titers assessed using double agar overlay plaque assay. The final preparation was completed with sterile water, resulting in a 1×10^8 PFU/mL titer. Inactive BAFASAL[®] (IBAF) was prepared by autoclaving this preparation at 120 °C for 30 min.

2.2. Stool Sample Preparation

The research ethics board protocol (#20160585-01H) for human stool sample collection was approved by the Ottawa Health Science Network Research Ethics Board at the Ottawa Hospital. Stool samples were obtained from five healthy volunteers (age range 27–36 years; three men and two women). Exclusion criteria for participation were irritable bowel syndrome, inflammatory bowel disease, or diabetes diagnosis; antibiotic use or gastroenteritis episode in three months preceding collection; use of pro-/pre-biotic, laxative, or anti-diarrheal drugs in the last month preceding collection; or pregnancy. Participants collected stool into a 50-mL Falcon tube containing 15 mL of sterile phosphate-buffered saline (PBS; pH 7.6) and 10% (v/v) glycerol pre-reduced with 0.1% (w/v) L-cysteine hydrochloride. Samples were weighed, transferred into an anaerobic workstation (5% H₂, 5% CO₂, and 90% N₂ at 37 °C), homogenized to 20% (w/v) in the same pre-reduced buffer mixture, and filtered using sterile gauzes to remove large particles to obtain the fecal inocula. Fecal inocula, as proxies for gut microbiomes, were stored at −80 °C until used in RapidAIM.

2.3. Culturing of Microbiota and Treatments

Fecal inocula were thawed at 37 °C and inoculated at a concentration of 2% (w/v) into a 96-well deep-well plate containing 1 mL MiPro optimized sterile and pre-reduced culture medium (2.0 g L^{−1} peptone water, 2.0 g L^{−1} yeast extract, 0.5 g L^{−1} L-cysteine hydrochloride, 2 mL L^{−1} Tween 80, 5 mg L^{−1} hemin, 10 μL L^{−1} vitamin K1, 1.0 g L^{−1} NaCl, 0.4 g L^{−1} K₂HPO₄, 0.4 g L^{−1} KH₂PO₄, 0.1 g L^{−1} MgSO₄·7H₂O, 0.1 g L^{−1} CaCl₂·2H₂O, 4.0 g L^{−1} NaHCO₃, 4.0 g L^{−1} porcine gastric mucin, 0.25 g L^{−1} sodium cholate, and 0.25 g L^{−1} sodium chenodeoxycholate), as per Li et al., in an anaerobic workstation [20,21]. BAF and IBAF were added at 2% (v/v) and 5% (v/v) to the media. For BAF, this equated to 2×10^6 and 5×10^6 PFU/mL, respectively. Fructo-oligosaccharide (FOS) is an oligosaccharide that is widely used as a prebiotic, and several studies document its effects on gut microbiome composition and function from both mice [22,23] and humans [24–26]. With consistent changes in composition, such as increases in *Bifidobacteria*, we utilized FOS as a positive control in our RapidAIM assay. It was added at 2% (v/v) and 5% (v/v) from a 250 mg/mL stock as a positive control and PBS (1×; pH 7.6) added as vehicle control at 2% (v/v) and 5% (v/v). Following the addition of inoculants and compounds, the plates were covered with vented sterile silicone mats and shaken at 500 rpm with a digital shaker (MS3, IKA, Germany) at 37 °C for 18 h in the anaerobic chamber. Treatments were randomized on the 96-well plates for each participant.

2.4. Sample Processing

Sample processing was done as per our reported sample processing workflows [20,21,27]. Briefly, following 18 h of culturing, samples were transferred from 96-well plates to individual 1.5-mL Eppendorf tubes. Sample order were randomized for processing. Samples were transferred out of the anaerobic station onto ice and centrifuged at $14,000\times g$ at $4\text{ }^{\circ}\text{C}$ for 20 min to pellet the microbiota. Supernatants were removed, and the pellets were resuspended in 1 mL cold $1\times$ PBS (pH 7.6). They were subsequently centrifuged at $300\times g$ at $4\text{ }^{\circ}\text{C}$ for 5 min to remove debris. With samples on ice, supernatants were transferred into new 1.5-mL Eppendorf tubes for two additional rounds of debris removal as above. Supernatants were transferred to 1.5-mL Eppendorf tubes and centrifuged at $14,000\times g$ at $4\text{ }^{\circ}\text{C}$ for 20 min to pellet the microbiota. Supernatants were removed, and the pelleted bacterial cells were resuspended and washed two times with 1 mL cold $1\times$ PBS (pH 7.6), pelleting the cells after each wash at $14,000\times g$ for 20 min at $4\text{ }^{\circ}\text{C}$. Before the final spin, resuspended bacterial samples were equally divided into new 1.5-mL Eppendorf tubes. Harvested bacterial cell pellets were stored at $-80\text{ }^{\circ}\text{C}$ prior to protein extraction or DNA extraction.

2.5. Metaproteomic Sample Processing and LS-MS/MS Analyses

Microbial pellets were resuspended in 100 μL of 8 M urea and 4% (*w/v*) sodium dodecyl sulfate (SDS) in 100 mM Tris-HCl (pH 8.0) plus Roche cOmplete™ Mini tablets. Lysis was completed with sonication (Q700 Qsonica, Newtown, CT, USA) at $8\text{ }^{\circ}\text{C}$, 50% amplitude (15.6 watts/sample), and sixty cycles of 10 s ultrasonication and 10 s cooling down. Samples were centrifuged at $16,000\times g$ for 10 min at $9\text{ }^{\circ}\text{C}$. Supernatants were transferred to new 1.5-mL Eppendorf tubes, and proteins in the supernatant were precipitated with $5\times$ volume of ice-cold protein precipitation buffer (acidified acetone/ethanol) overnight at $-20\text{ }^{\circ}\text{C}$. Proteins were pelleted by centrifugation at $16,000\times g$ for 20 min at $4\text{ }^{\circ}\text{C}$ and washed $3\times$ in ice-cold acetone. Proteins were resuspended in 100 μL of 6 M urea in 50 mM ammonium bicarbonate (ABC; pH 8.0), with sonication as above. Protein concentrations were measured in triplicate using Bio-Rad's detergent compatible, DC Protein Assay (USA). Trypsin digestion was carried out as described in Zhang et al. [28]. For each sample, 50 μg of protein was reduced with 10 mM dithiothreitol (DTT) at $56\text{ }^{\circ}\text{C}$ for 30 min and alkylated in the dark with 20 mM iodoacetamide (IAA) at room temperature for 45 min, followed by $10\times$ dilution into 50 mM ABC (pH 8.0) and tryptic digestion at $37\text{ }^{\circ}\text{C}$ for 20 h with shaking using 1 μg of trypsin (Worthington Biochemical Corp., Lakewood, NJ, USA) per 50 μg protein. Trypsin digestion was stopped by addition of 10% (*v/v*) formic acid (FA) to pH 2–3. Acidified, digested peptides were desalted using 10 μm C18 column beads, according to our laboratory standard protocol [20], dried via vacuum centrifugation, and resuspended in 100 μL 0.1% (*v/v*) FA for tandem mass spectrometry (MS/MS) analyses. As quality control (QC) samples to be assessed repeatedly throughout our MS/MS runs, 10 peptide samples were selected at random and combined. Two microlitres (1 μg peptides) were loaded in a randomized order for liquid chromatography tandem mass spectrometry (LC-MS/MS) onto an Agilent 1100 Capillary LC system (Agilent Technologies, San Jose, CA) and a Q Exactive mass spectrometer (ThermoFisher Scientific Inc.). Peptides were separated on a tip column (75 μm inner diameter \times 50 cm) packed with reverse phase beads (1.9 $\mu\text{m}/120\text{ \AA}$ ReproSil-Pur C18 resin, Dr. Maisch GmbH, Ammerbuch, Germany) using a 90-min gradient from 5 to 30% (*v/v*) acetonitrile at a 200 nL/min flow rate. A total of 0.1% (*v/v*) FA in water was used as solvent A, and 0.1% FA in 80% acetonitrile was used as solvent B. The MS scan was performed from 300 to 1800 *m/z*, followed by data-dependent MS/MS scans of the 12 most intense ions, a dynamic exclusion repeat count of two, and repeat exclusion duration of 30 s were used. The resolutions for MS and MS/MS were 70,000 and 17,500, respectively.

2.6. Metaproteomic Data Analysis

Mass spectrometry proteomics data were deposited on 8 July 2021 to the ProteomeX-change Consortium (<http://www.proteomexchange.org>) via the PRIDE partner repository

with the data identifier PXD027172. Peptide/protein identification and quantification, taxonomic assignment, and functional annotations were done using MetaLab (version 1.1.0) [29]. Briefly, MetaLab automates an iterative database search strategy called MetaPro-IQ, described in Zhang et al. (2016). The MetaPro-IQ search was based on a human gut microbial gene catalog containing 9,878,647 sequences from https://db.cngb.org/microbiome/genecatalog/genecatalog_human/. In MetaLab, a spectral clustering strategy [29] was used for database construction from all raw files. Then the peptide and protein lists were generated by applying strict filtering based on a false-discovery rate (FDR) of 0.01, and quantitative information for proteins was obtained with the maxLFQ (label-free quantification) algorithm on MaxQuant (version 1.5.3.30). Carbamidomethyl (C) was set as a fixed modification, and oxidation (M) and N-terminal acetylation (Protein N-term) were set as variable modifications. The matching between runs option was used. Instrument resolution was set as “High-High”. Quantified protein groups were filtered according to the criteria that the protein appeared in >50% of the gut microbiomes for each treatment. Protein group LFQ intensities were then log₂-transformed. Functional annotations of protein groups, including COG (Clusters of Orthologous Groups) information, were obtained using MetaLab. Functional responses, including hierarchical clustering, heatmaps, and principal component analyses (PCA), were analyzed and visualized using R (version 4.0.2) or Shiny apps on imetalab.ca.

2.7. Metagenomic DNA Extraction and 16S rDNA-V4 Amplicon Sequencing

Metagenomic DNA extraction from samples (RapidAIM cultures and stools) and V4-16S rRNA gene library construction and sequencing were done as previously described [30,31]. Samples were extracted in the same randomized order as in the metaproteomic analysis. Briefly, metagenomic DNA was extracted using beads beating, extracted DNA normalized, and the V4-16S rRNA gene PCR amplified. Positive controls included a ZymoBiotics community standard (Cat# D6300) that was processed alongside the study samples. Negative controls included extraction blanks and RT-PCR grade water (Ambion Cat#: AM9935) as the template for the V4-16S rRNA PCR. We processed BAF and IBAF preparations through our extraction/sequencing pipeline and also used pure BAF/IBAF as a template to our V4 amplicon PCR to identify potential contaminating bacteria in the BAF/IBAF preparations. V4 PCR amplicons were normalized by mass, pooled together, sized selected, and quantified using an Agilent Bioanalyzer. The pooled library was subsequently templated and sequenced using an IonChef and Ion Torrent Proton sequencer using the manufacturer’s recommended protocol. The samples were partitioned between the two sequencing chips in a randomized fashion. Two separate V4-16S rRNA amplicon libraries were constructed for the input stool samples and included on each sequencing chip to assess reproducibility.

2.8. Processing for 16S rRNA Sequencing and Analyses

Raw sequencing reads were quality filtered and demultiplexed prior to OTU (operational taxonomic unit) picking, as previously described. The demultiplexed reads were deposited on 14 July 2021 and are available at the NCBI Sequence Read Archive (<http://www.ncbi.nlm.nih.gov/sra>) under ascension PRJNA746541. QIIME 1.9.1 was used to identify OTUs using a closed-reference strategy against the SILVA 119 database, and the resulting data analyzed in R. Potential contaminants were removed with the decontm package using V4 amplicon concentrations prior to pooling. OTUs were subsequently filtered to only keep those with ≥ 2 counts at least 5% of the final sample dataset, and samples were rarefied to 90,000 reads prior to analysis. Samples with less than 90,000 reads were discarded. Differences in alpha diversities (Chao1 index and Shannon diversity) were assessed using a Kruskal–Wallis test with Dunn’s post-hoc test. Beta diversities were assessed using the Bray–Curtis dissimilarity, weighted Unifrac distance, and unweighted Unifrac distance. The impact of BAF or IBAF on beta diversity clustering was assessed with adonis function from vegan by pooling the samples for each stool donor. Potentially differentially abundant taxa between the PBS and BAF/IBAF cultures were assessed using

MaAsLin2 controlling for stool donors using the default parameters. Results were considered significant with a p -value < 0.05 and, where appropriate, after controlling for multiple hypothesis testing using the Benjamini and Hochberg approach.

3. Results

3.1. Experimental Set-Up

In this study, we used our well-established and optimized RapidAIM (Rapid assay of an individual microbiome) workflow to carry out both metaproteomic and metagenomic analyses of five human gut microbiomes following in-vitro treatment with the BAFASAL[®] commercial bacteriophage mixture (Figure 1). Microbiotas were harvested from the feces of five participants (three men and two women) as proxies of their gut microbiota. In brief, microbiota samples were derived from homogenized human feces and stabilized in 20% (w/v) anaerobic, pre-reduced $1\times$ PBS/10% (v/v) glycerol/0.1% (w/v) L-cysteine. These samples were inoculated to 2% (w/v) in 1 mL of Mi-Pro optimized culture media and incubated under anaerobic conditions at 37 °C for 18 h. We have shown that this in-vitro assay maintains both gut microbiome composition and function over 24 h in culture [21]. To evaluate the potential effects of BAFASAL[®] on human gut microbiota, we compared (1) BAFASAL[®]-treated microbiota (BAF) to those microbiotas exposed to (2) heat-inactivated BAFASAL[®] (IBAF), (3) positive control fructo-oligosaccharide (FOS), and (4) vehicle phosphate-buffered saline (PBS; pH 7.6). Samples were cultured in triplicate for each condition and at 2% (v/v) and 5% (v/v) concentrations, as described in materials and methods. Following 18 h culturing, the bacterial cells were pelleted, DNA extracted for metagenomic analyses using 16S rRNA gene-based sequencing, and proteins extracted and digested for metaproteomic analysis, as described in materials and methods. We used 16S rRNA gene amplicon data to analyze compositional changes and metaproteomics to focus on functional changes following gut microbiome treatments.

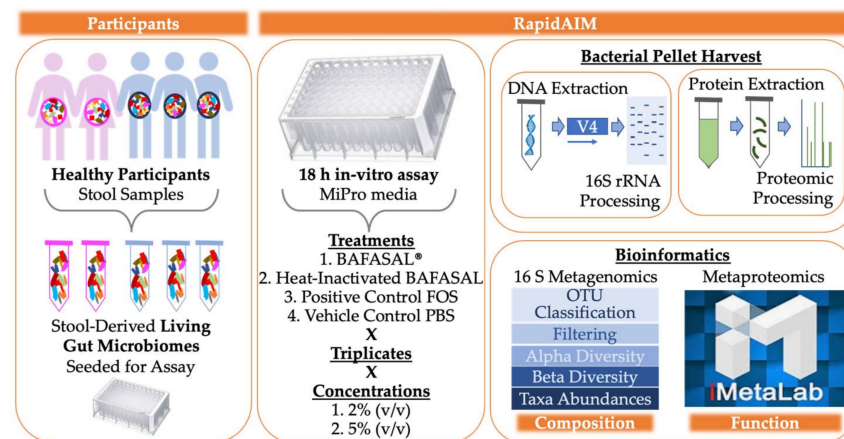


Figure 1. Experimental Set-Up. Microbiotas were harvested from the feces of five participants (3 men and 2 women) as proxies of their gut microbiota. Samples were derived from homogenized human feces stabilized in 20% (w/v) anaerobic, pre-reduced $1\times$ PBS/10% (v/v) glycerol/0.1% (w/v) L-cysteine. Samples were inoculated to 2% (w/v) in 1 mL of Mi-Pro optimized culture media and incubated under anaerobic conditions at 37 °C for 18 h. To evaluate the potential effects of BAFASAL[®] on human gut microbiota, we compared (1) BAFASAL[®]-treated microbiota (BAF) to those microbiotas exposed to (2) heat-inactivated BAFASAL[®] (IBAF), (3) fructo-oligosaccharides as a positive control (FOS), and (4) phosphate-buffered saline (PBS; pH 7.6) as a negative control in triplicate and at two concentrations, as defined in materials and methods. Following culturing, microbial cells were pelleted and frozen until further analysis. DNA was extracted for metagenomic analyses using 16S rRNA gene-based sequencing and proteins extracted and digested for metaproteomic analysis, as described in materials and methods. Bioinformatic analysis was used to determine gut microbiome compositional and functional changes in response to treatment.

3.2. Microbial Biomass

We firstly assessed whether BAFASAL[®] addition would impact the ability of human microbiotas to grow in-vitro. As a gross measure for tracking increases in microbial biomass, we measured the amount of metagenomic DNA extracted for each individual under the different treatments (Figure 2). For all individuals, biomass did not differ following either BAF or IBAF treatments. Nor did these treatments differ when compared to the PBS vehicle control for our positive treatment FOS. In contrast, almost all individuals showed reduced bacterial biomass upon FOS treatment. This biomass reduction is likely due to the production of short-chain fatty acids that acidified the medium and inhibited specific microbes' growth.

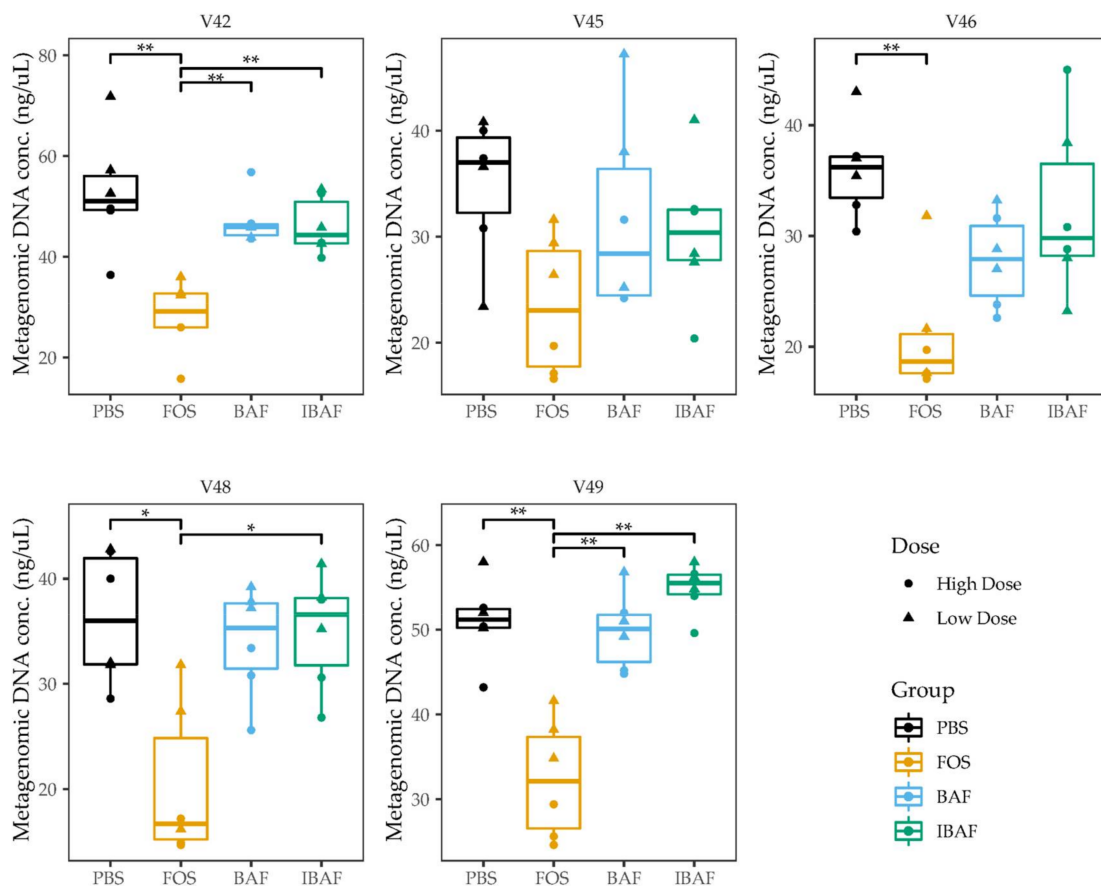


Figure 2. BAFASAL[®] treatment does not impact microbial biomass after 18 h of in-vitro growth. Microbial biomass expressed as the quantity of metagenomic DNA (ng/uL) extracted for each donor and each treatment. Donors are plotted separately, and the high/low treatments combined. Statistical differences were assessed using Kruskal–Wallis test with Dunn's multiple comparison post-hoc test. * $p < 0.05$, ** $p < 0.01$.

3.3. Compositional Analyses

3.3.1. RapidAIM and Sequencing Library Reproducibility

We assessed the reproducibility of the sequencing reactions by comparing the human gut microbiome profiles of the stool samples that were sequenced on both chips for high and low doses. Principal coordinate analysis (PCoA) using the Bray–Curtis dissimilarity revealed that the individual stools clustered tightly together in a donor-dependent manner (Figure S1A) with essentially no separation between the two sequencing chips. Moreover, we assessed the reproducibility of the RapidAIM culturing assay by comparing the PBS replicates between the high/low dose conditions, as these would be expected to show few differences. This analysis revealed little separation between the two culturing conditions (Figure S1B), with the samples again segregating primarily by an individual. Finally, our

commercial standards revealed that we could detect all the genus present in this mix and could distinguish between the closely related *Escherichia coli* and *Salmonella enterica* present in the standard (Figure S1C).

3.3.2. Microbial Diversity Analyses

We next evaluated whether BAFASAL[®] impacted microbial alpha diversity. Species richness (Figure 3A) and diversity (Figure 3B) did not differ significantly among BAF, IBAF, and PBS treatments at either dosing level. Treatment with FOS lowered the overall diversity at high concentrations but had no impact on overall species richness.

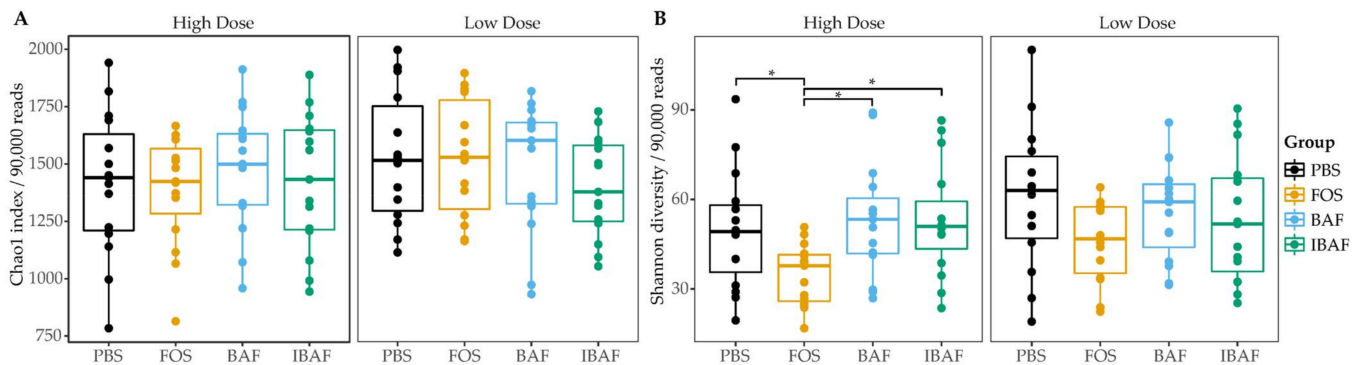


Figure 3. BAFASAL[®] treatment does not impact microbial alpha diversity. Species richness (A) and diversity (B) were assessed for each treatment group. There was no difference in between the groups except for lowered species diversity in the high FOS concentration. Statistical differences assessed using a Kruskal–Wallis test with Dunn post-hoc test. * $p < 0.05$.

We subsequently compared the microbiota beta diversity profile for all RapidAIM assayed samples (BAF, IBAF, PBS, and FOS, at both high and low doses; Figure 4). This analysis revealed that samples from a given individual formed their own cluster regardless of treatment, underscoring each individual's highly personalized microbiota and the need to assess microbial responses on a personalized level.

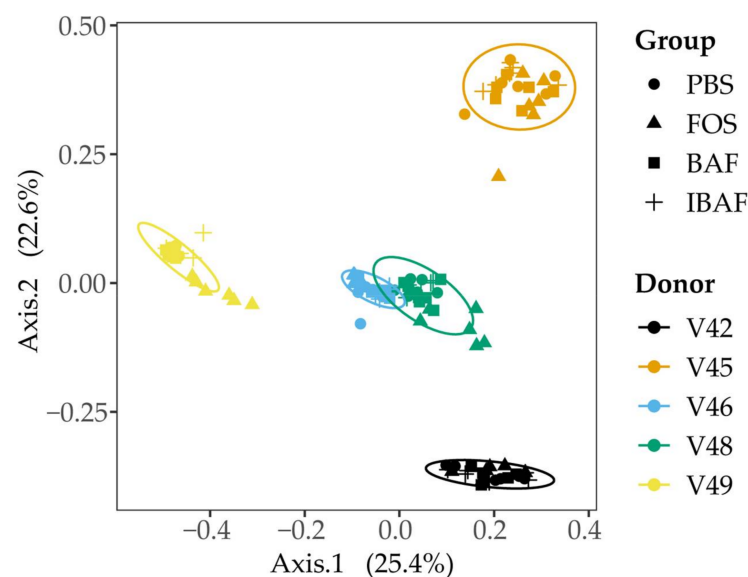


Figure 4. Principal coordinate analysis of the RapidAIM cultures reveal the highly personalized nature of human gut microbiomes. All RapidAIM assay microbiota results were analyzed using Principal coordinate analysis of the Bray–Curtis dissimilarity. This analysis revealed that each donor formed its own cluster, demonstrating the highly personalized nature of human gut microbiomes and the requirement for high-throughput in-vitro assays to assess microbial responses on a personalized level.

Comparing the microbiota profiles for each individual's treatments separately revealed that BAF and IBAF treatments did not result in major changes in the overall microbial community for any of the participants (Figure 5). This is in contrast with FOS treatment, which resulted in clear shifts in microbiota community composition for each individual. Notably, the lack of separation between the BAF, IBAF, and PBS communities persisted even after removing the FOS samples (Figure S2) or when assessing the microbial communities using either weighted or unweighted Unifrac distances (data not shown).

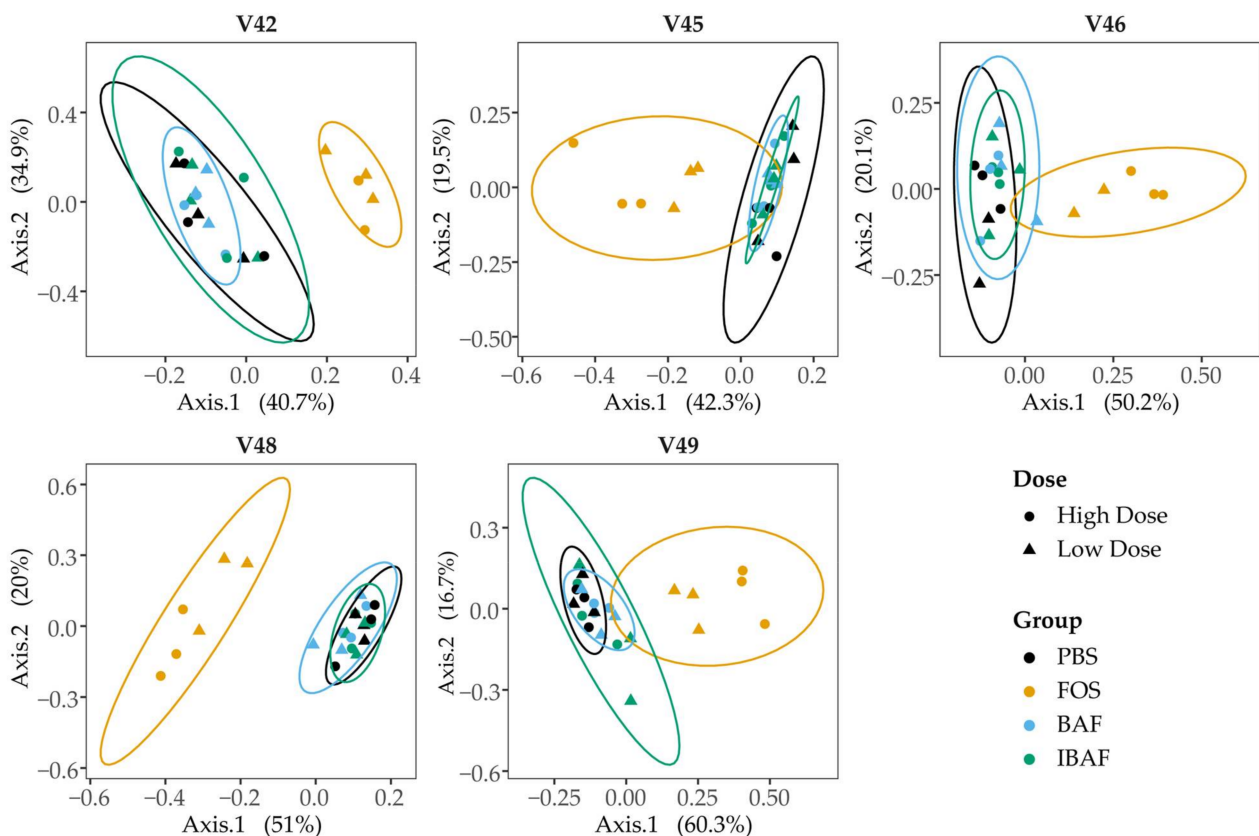


Figure 5. Principal coordinate analysis of RapidAIM cultures from each donor reveals that BAFASAL[®] treatment has minimal impact on microbial composition. RapidAIM assays from each donor were analyzed separately using principal coordinate analysis of the Bray–Curtis dissimilarity and plotted as separate panels. This analysis reveals the large impact that FOS treatment has on patient microbiotas that could be obscured by high interpatient variability (Figure 4). There were no apparent differences between the PBS and BAFASAL[®]/inactivated BAFASAL[®] treatments.

3.3.3. Compositional Differences

We could not identify significantly differentially abundant taxa between the BAF-, IBAF-, and PBS-treated samples. This was true whether analyzing the high and low dosing regimens separately or by pooling the two dosing groups together. As BAF specifically targets *Salmonella*, we then focused on the abundances of related genera in the Enterobacteriaceae family. There were no apparent differences between the dominant Enterobacteriaceae genera in the BAF-, IBAF-, and PBS-treated cultures (Figure S3). In contrast with the above results, there were differences between the PBS- and FOS-treated samples that mirror previously reported results, such as increased *Bifidobacteria* genera (data not shown). Notably, and as expected, FOS treatment reduced the levels of several Enterobacteriaceae family members, such as *Escherichia* genera.

3.4. Functional Analyses

Metaproteomic functional analyses were based on data from the MS/MS spectra collected with an average identification rate of 40.77%, with 1,364,000 MS/MS submitted

and 556,283 identified. In total, 65,760 peptides were identified and quantified that mapped to 16,064 proteins across the 60 samples.

3.4.1. Metaproteomic Assessed Responses to BAFASAL[®]

To examine similarities and differences in protein expression following BAF, IBAF, PBS, and FOS treatments of the five human gut microbiomes, we applied hierarchical cluster analyses for proteins identified in >50% of all samples (Q50) (Figure S4, Panels A (low dose) and B (high dose)). As expected, quality control (QC) samples clustered together. While an individual's gut microbiome samples clustered together, clustering did not occur among BAF-, IBAF-, and PBS-treated gut microbiomes for an individual's samples at either dose. Meanwhile, our FOS positive control induced significant shifts in protein abundances for each individual's gut microbiome, resulting in their clustering at both low and high doses. In fact, high-dose FOS treatment shifted protein expression patterns such that FOS-treated gut microbiomes between individuals clustered together and moved further away from their corresponding control-treated PBS gut microbiomes (Panel B).

Principal component analysis (PCA) of those quantified protein groups (Q50) revealed that gut microbiome samples from an individual clustered together, showing again interindividual gut microbiome differences (Figure 6). No clustering occurred among BAF-, IBAF-, and PBS-treated gut microbiomes for any individual and at either low (Panel A) or high (Panel B) doses while QC samples clustered tightly. At low dose, FOS-treated gut microbiomes formed a sub-cluster within an individual's larger cluster (Panel A). At higher doses an individual's sample treated with FOS separated from its BAF-, IBAF- and PBS-treated samples along principal component axis 1, again indicating the variations induced by high-dose FOS treatments were greater than gut intermicrobiome variations (Panel B).

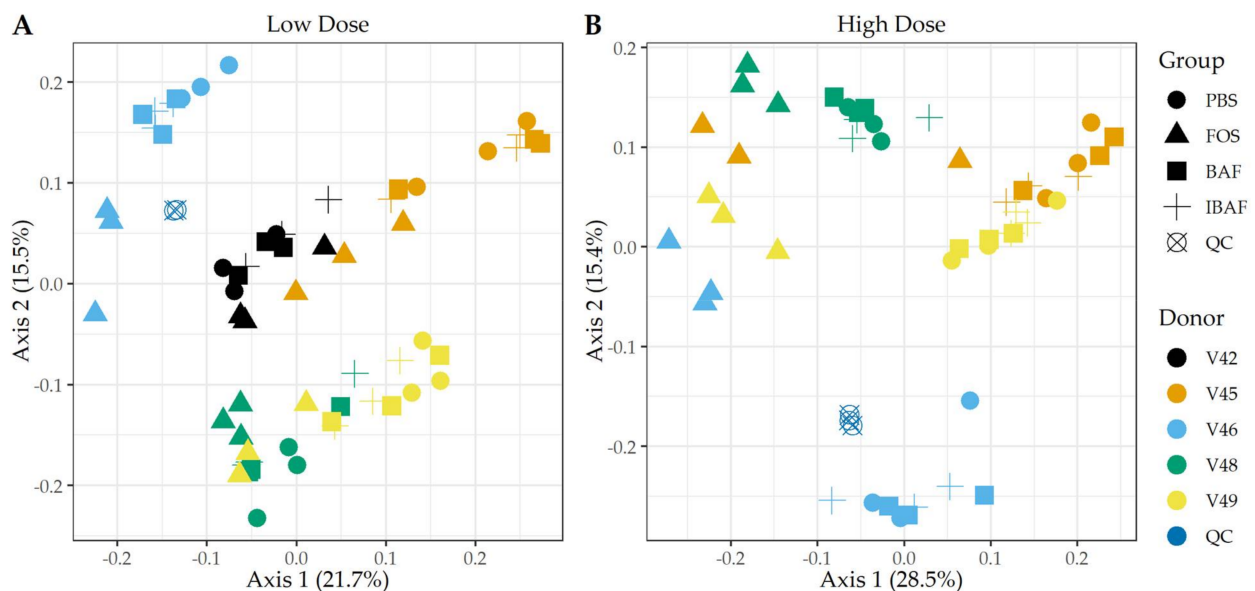


Figure 6. Principal component analyses of protein groups demonstrate the unique pattern of an individual's protein expression profile and absence of BAFASAL[®] impact. Panels A,B show principal component analyses (PCA) at the protein level per sample and for low and high doses, respectively. Colors indicate volunteer samples and shapes treatment as shown to legends on the right of each panel. Note: Only those protein groups that have non-zero values in >50% of samples were used for analyses (Q50).

3.4.2. Functional Responses to BAFASAL[®]

We studied the functional distribution of identified human gut microbiome proteins and any changes induced with treatment via functional hierarchical clustering (Figure S5)

and PCA (Figure 7). Functional annotation of the protein groups using Clusters of Orthologous Groups (COGs) database did not reveal functional changes among BAF-, IBAF-, and PBS-treated gut microbiomes for an individual and at either low (Panels A) or high dose (Panels B) treatment. Quality control samples clustered tightly together, as expected. Similar to clustering observed for protein-level analyses, at low doses, FOS-treated gut microbiomes formed a sub-cluster usually within an individual's cluster (Figure 7, Panel A). Samples treated with FOS at higher doses separated from other samples along principal component axis 1, indicating again that the functional variations induced by high-dose FOS were greater than gut intermicrobiome functional variations (Figure 7, Panel B).

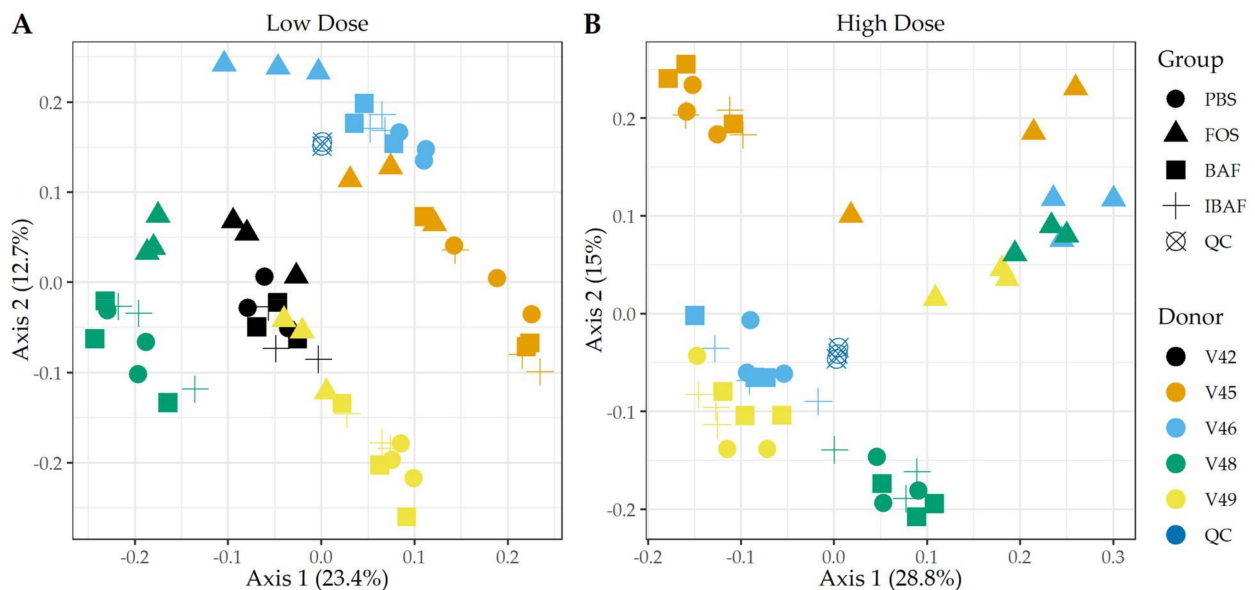


Figure 7. Principal component analyses of clusters of orthologous groups (COGs) demonstrate the unique pattern of an individual's functional metaproteomic profile and absence of BAFASAL[®] impact. Principal Component Analyses—COGs. Panels A,B show principal component analyses (PCA) using COGs per sample and for low and high doses, respectively. Colors indicate volunteer samples and shapes treatment as shown to legends on the right of each panel. Note: Only those COGs that have non-zero values in >50% of samples were used for analyses (Q50).

Supplemental Figures 6–8 illustrate the abundance distribution of major functional categories, including translation, amino acid metabolism, carbohydrate metabolism, lipid metabolism, and energy metabolism. There were no significant changes for any individual nor dosage when comparing BAF-, IBAF-, and PBS-treated gut microbiomes for diverse COGs, such as translation, ribosomal structure, and biogenesis; amino acid transport and metabolism; lipid transport and metabolism; nucleotide transport and metabolism; carbohydrate transport and metabolism; and energy production and conversion. In contrast, the FOS positive control had significant effects on multiple COG categories, including increased functional categories of translation and amino acid metabolism; decreased lipid transport and metabolism; increased nucleotide transport and metabolism; increased carbohydrate transport and metabolism, and increased energy production and conversion, all at low and high doses with inter-individual variation and responses.

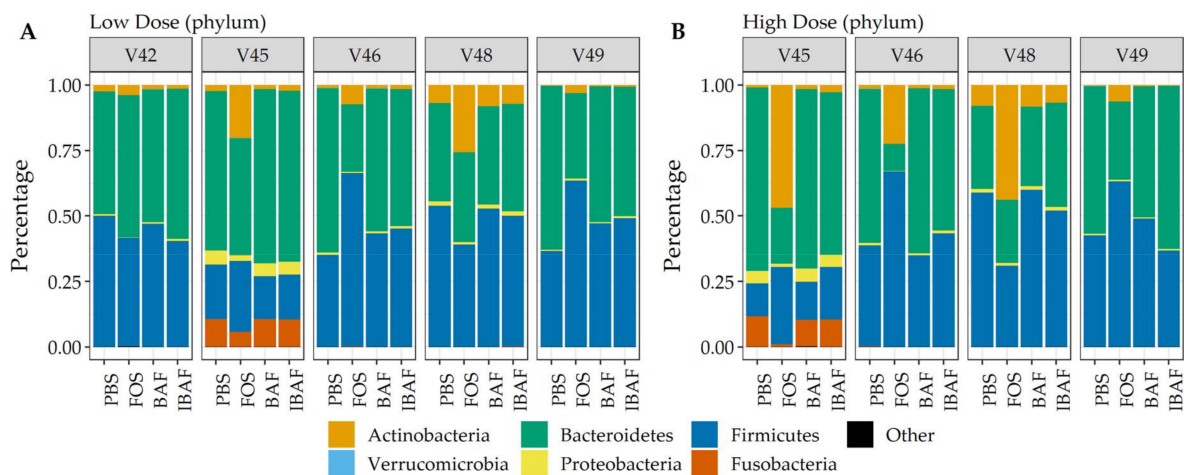


Figure 8. Taxonomic analyses at the phylum level demonstrates the unique composition of an individual's gut microbiome via metaproteomic profiling and absence of BAFASAL[®] impact. Stacked bar representation from label-free quantification of protein groups assigned to phylum (Panel (A), low dose, and Panel (B), high dose) expressed as percentages. Individual gut microbiomes are grouped, and the phylum are identified by colored bars, as indicated in key below panels.

3.5. Metaproteomic Comparative Taxonomic Analyses

Additionally, and complementing our 16S analyses, we performed comparative taxonomic analyses at phylum (Figure 8) and genus levels (Figure 9) using quantified peptides in metaproteomics. No phylum-level changes were observed at either low (Panel A) or high (Panel B) doses among BAF-, IBAF-, and PBS-treated gut microbiomes for an individual (Figure 8). Several phyla abundances were significantly increased in FOS-treated versus vehicle PBS-treated gut microbiomes, including Actinobacteria, as expected and documented in the literature [22]. Similarly, no obvious genus-level changes were observed at either low (Panel A) or high (Panel B) doses among BAF-, IBAF-, and PBS-treated gut microbiomes for an individual (Figure 9). However, FOS treatment increased *Bifidobacterium* as expected and documented in the literature [22].

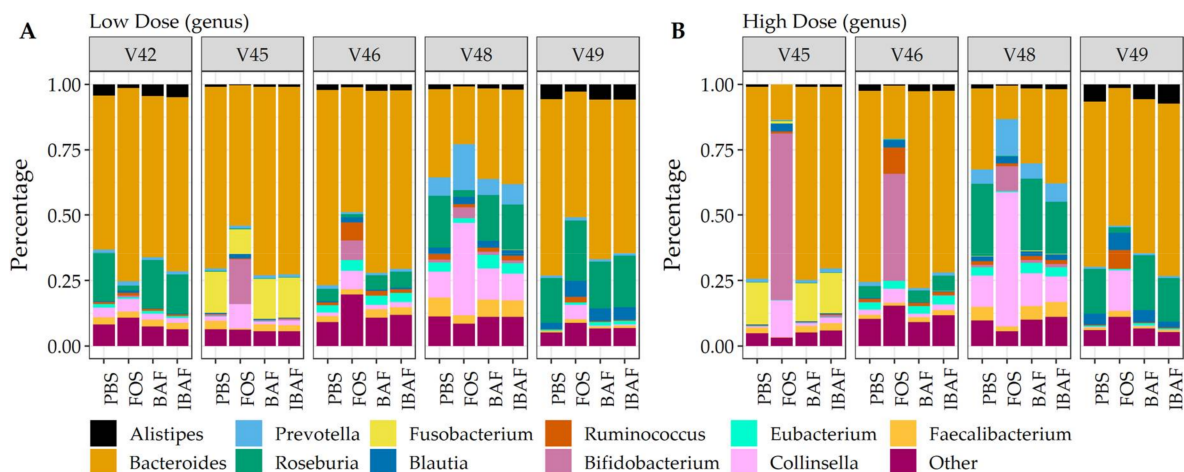


Figure 9. Taxonomic analyses at the genus level demonstrates the unique composition of an individual's gut microbiome via metaproteomic profiling and absence of BAFASAL[®] impact. Stacked bar representation from label-free quantification of protein groups assigned to genus (Panel (A), low dose, and Panel (B), high dose) expressed as percentages. Individual gut microbiomes are grouped, and the top 11 genus are identified by colored bars as indicated in key below panels.

4. Discussion

This study aimed to examine the effects of the BAFASAL[®] agricultural bacteriophage mixture on human gut microbiome function and composition using an in-vitro RapidAIM platform. In particular, we were interested in whether this agricultural bacteriophage mixture, used as a feed additive in poultry farming to prevent and eliminate *Salmonella*, would display off-target effects on the human gut microbiome. It has been reported that BAFASAL[®] significantly reduces *Salmonella* levels in poultry, reducing mortality and improving feed conversion rates [12]. These types of therapeutic and prophylactic agricultural bacteriophages are important tools to address the critical, on-going need to maintain food safety, improve the health of animals in our food chains, and reduce human morbidity and mortality due to consumption of contaminated food. Bacteriophage development and studies regarding their safe introduction into our food chain have been prompted in light of growing antimicrobial resistance and the environmental pollution caused by decades-long, wide-spread antibiotic use in the food industry [4].

Bacteriophages, as self-replicating and self-limiting agents, are generally regarded as safe. A bacteriophage preys on specific bacterial strains due to their specificity in recognizing particular receptors on target bacteria [7]. Additionally, virulent bacteriophages that exhibit only a lytic mechanism of replication, of which BAFASAL[®] is composed, are desirable as therapeutics since once their target bacteria are infected and lysed, the bacteriophages themselves become self-limiting. To date, rodent models have been used extensively to examine bacteriophage safety as therapeutics in medicine and agriculture. Oral administration of different anti-*Salmonella* bacteriophage mixtures into mice did not result in gross clinical changes or mortality [12,32]. Additionally, mice treated with a bacteriophage therapeutic against *E.coli* also did not exhibit any toxic effects [33].

Herein, we determined whether the bacteriophage mixture BAFASAL[®], proven effective against *Salmonella* sp. in poultry, would affect the human gut microbiome using our novel multi-omics RapidAIM approach against healthy adult gut microbiomes. The 16S rRNA gene sequencing captured compositional changes and was complemented by proteomics analyses that, in addition to providing confirmatory information on taxonomic abundances, can accurately quantify expressed proteins and assess functional changes. It was important to use both approaches, as our previous work demonstrated that bacterial function could change and shift in response to a stimulant without a change in the abundance of bacteria [20].

As a gross measure of BAF potential impact on gut microbiota, we showed that total biomass was unaffected compared to IBAF-treated gut microbiomes (Figure 2). Nor did it differ from our PBS-treated negative control. In contrast, FOS-treated gut microbiome biomasses were lower than all other groups, suggesting FOS treatment depresses selective or general gut bacterial growth. Microbial richness and diversity were unaffected by BAF treatments (Figure 3), while FOS treatment reduced microbial richness, likely due to specific microbes thriving when using this carbon source and suppressing the growth of competitors. Similarly, only FOS significantly affected beta-diversity metrics for each individual gut microbiome, while BAF-treated gut microbiomes were indistinguishable from their corresponding heat-inactivated and PBS-treated gut microbiomes (Figures 4 and 5). Overall, metagenomics using 16S rRNA amplicon analyses did not reveal significant changes in the composition or abundances of the gut microbiomes obtained from any of the five healthy adults following 18-h culture with BAF at two concentrations in comparison to IBAF or PBS. These results differed from the FOS positive control, which resulted in the expected and documented increases in *Bifidobacteria* genera and reduced levels of several Enterobacteriaceae family members (Figure S3) [22,23].

Hierarchical clustering of microbial proteins did not reveal shifts in protein abundances among BAF, IBAF, and PBS treatments at either dose for any individual gut microbiome tested, while FOS treatment induced changes in protein expression so that these samples clustered at both low and high doses. In fact, at high dose, FOS treatment protein-abundance changes overcame intraindividual clustering (Figure S4). Likewise,

PCA analyses did not detect any shifts in protein differences in BAF, IBAF, and PBS treatments at either dose, while low-dose, FOS-treated gut microbiomes separated from their individual gut microbiome, and at high dose, those FOS-induced changes were increased to the level that would overcome interindividual differences (Figure 6). Collectively, these analyses did not reveal any significant shifts in protein abundance with BAF treatment. Results from FOS treatments established the utility of the metaproteomic branch of the RapidAIM assay to reliably and reproducibly detect expressed protein-abundance changes and that dose-dependent effects can be measured and differentiated. Quantified protein groups were assigned to functional pathways to examine whether microbial function differs with BAF treatment (Figure 7). There were no differences detected under BAF treatment (Figures S6–S8), while FOS-treated gut microbiomes show predicted changes from past metagenomic studies [22,23]. Metaproteomic assessment of phylum- and genus-level abundances in the presence of BAF treatment were similar to IBAF- and PBS-treated gut microbiomes. Overall, metaproteomic analyses did not reveal obvious protein abundance changes nor functional changes of the gut microbiomes obtained from any of the five healthy adults following 18-h culture with BAF at two concentrations and in comparison to IBAF or PBS. Meanwhile, our control FOS showed the expected and documented changes, such as increases in *Actinobacteria* and decreases in *Proteobacteria* (Figures 8 and 9) [22,23].

The gut microbiome composition of humans has a definite impact on health and disease. The gut is an important milieu where the host, pathogens, and foods interact. Shifts in our gut microbiome due to diet, treatments, therapies, and antibiotics can be correlated with diseases. As such, food industry leaders and government regulators are closely studying the impact of food processing, additives, etc., on the gut microbiome. Antibiotics, especially broad-spectrum antibiotics, have profound effects on the gut microbiota. We have recapitulated and documented these effects previously using the RapidAIM platform [20]. Bacteriophages are very abundant in human guts as stable members of our niche microbiota, with estimates of 10^{12} bacteriophages per gram found in our feces. Many are lysogenic phages, and replication only occurs in their bacterial hosts. Nonetheless, it is vital to understand whether bacteriophages introduced and used as therapies in, for instance, agriculture, could make their way into the human intestinal system and have significant off-target effects. Agricultural workers may be uniquely at risk for any effects of these new therapies and prophylactics as they may be exposed to agricultural residues with residual bacteriophage from the feed.

The RapidAIM platform as utilized in this study provided an opportunity to investigate the effects of the bacteriophage mixture BAFASAL[®] on human gut microbiota and on an individual basis. To our knowledge, this is the first study of this kind to measure the response of the human gut microbiome to a bacteriophage-based product. That we measured responses on an individual basis is a strength of this in-vitro assay, as studies show our gut microbiomes are as unique as their hosts and can respond differentially to stimuli. Indeed, we have previously shown how individual gut microbiomes vary in their response to drug treatments [20]. As well, we used a multi-omics approach employing both 16S rRNA gene sequencing and metaproteomics to investigate the effects of BAFASAL[®] on both human gut microbiome composition and function. Notably, the RapidAIM platform is amenable to metabolomics that could be advantageous in future studies, providing additional information on the functional capacity of a microbiome and the effects of stimulation/treatment. Technologies such as single amplified genome (SAG) sequencing could be used following RapidAIM to identify responders at the species level. This has been successfully employed in mice to identify insulin responders from their gut microbiota [34]. Finally, we examined five individual gut microbiomes' responses to BAFASAL[®] in this pioneering study; however, the RapidAIM platform is scalable to a large number of individuals, can be modified for pooled effects, and can simultaneously screen large numbers of compounds. In this study, we utilized the RapidAIM platform and demonstrated that BAFASAL[®] did not affect gut microbiome composition nor gut

microbiome function from the five individual participants and suggested that results from such an assay can be added to therapeutic and prophylactic bacteriophage safety profiling.

5. Conclusions

The goal of our study was to utilize RapidAIM, a novel, in-vitro assay of the gut microbiome, to assess the effect of BAFASAL[®] bacteriophage preparation on our gut microbiota. In this multi-omics study, including 16S rRNA gene sequencing and metaproteomics, we showed that BAFASAL[®] does not affect healthy human adult gut microbiomes' composition and function. This study also highlights the value of the RapidAIM assay as a tool/platform to rapidly measure whether or not novel antibacterial solutions, including bacteriophage-based products, affect our niche gut microbiota ecology.

Supplementary Materials: The following are available online at <https://www.mdpi.com/article/10.3390/v13091734/s1>, Figure S1: RapidAIM assay and sequencing pipeline generate reproducible results; Figure S2: Principal coordinate analysis of RapidAIM cultures from each donor reveals that BAFASAL[®] treatment has minimal impact on microbial composition; Figure S3: BAFASAL[®] has no apparent impact on the abundances of Enterobacteriaceae genera; Figure S4: Sample clustering at the protein level does not support an effect for BAFASAL[®] on human gut microbiome protein expression; Figure S5: Sample clustering at the functional level does not support an effect for BAFASAL[®] on the human gut microbiome; Figure S6: Abundance distribution of major functional categories via clusters of orthologous groups (COGs) analyses for translation, ribosomal structure and biogenesis, and amino acid transport and metabolism; Figure S7: Abundance distribution of major functional categories via clusters of orthologous groups (COGs) analyses for lipid transport and metabolism and nucleotide transport and metabolism; Figure S8: Abundance distribution of major functional categories via clusters of orthologous groups (COGs) analyses for carbohydrate transport and metabolism and energy production and conversion.

Author Contributions: Conceptualization, D.F., A.S., E.W., J.D., J.M., X.Z., J.B. and Z.N.; methodology, J.M., X.Z., J.B., K.W. and Z.N.; software, X.Z., J.B. and Z.N.; validation, X.Z., J.B., J.M. and Z.N.; formal analysis, X.Z. and J.B.; investigation, J.M., X.Z., J.B., K.W. and Z.N.; resources, D.F., A.S., E.W. and J.D.; data curation, X.Z., J.B. and Z.N.; writing—original draft preparation, J.M.; writing—review and editing, D.F., A.S., E.W., J.D., J.M., K.W., X.Z., J.B. and Z.N.; visualization, X.Z., J.B. and J.M.; supervision, D.F. and A.S.; project administration, D.F., A.S. and J.M.; funding acquisition, D.F., A.S., E.W. and J.D. All authors have read and agreed to the published version of the manuscript.

Funding: This research received no external funding.

Institutional Review Board Statement: The research ethics board protocol (# 20160585-01H) for human stool sample collection was approved by the Ottawa Health Science Network Research Ethics Board at the Ottawa Hospital.

Informed Consent Statement: Informed consent was obtained from all subjects involved in the study.

Data Availability Statement: Mass spectrometry proteomics data were deposited to the ProteomeXchange Consortium via the PRIDE partner repository with the data identifier PXD027172. For 16S RNA sequencing, the demultiplexed reads are available at the NCBI Sequence Read Archive (<http://www.ncbi.nlm.nih.gov/sra>) under ascension PRJNA746541.

Acknowledgments: The authors wish to thank the volunteers who participated in this study.

Conflicts of Interest: D.F. and A.S. have co-founded MedBiome, a clinical microbiomics company. J.D. is a founder of the company Proteon Pharmaceuticals S.A., which developed the BAFASAL[®] preparation. All other authors declare no potential conflict of interest.

References

1. CDC Newsroom. 8 Zoonotic Diseases Shared Between Animals and People of Most Concern in the U.S. Centers for Disease Prevention and Control. 2019. Available online: <https://www.cdc.gov/media/releases/2019/s0506-zoonotic-diseases-shared.html> (accessed on 10 October 2020).
2. World Health Organization. Food Safety. 2020. Available online: <https://www.who.int/health-topics/food-safety/> (accessed on 10 October 2020).

3. van Boeckel, T.P.; Pires, J.; Silvester, R.; Zhao, C.; Song, J.; Criscuolo, N.G.; Gilbert, M.; Bonhoeffer, S.; Laxminarayan, R. Global trends in antimicrobial resistance in animals in low- and middle-income countries. *Science* **2019**, *365*, eaaw1944. [[CrossRef](#)]
4. Patel, S.J.; Wellington, M.; Shah, R.M.; Ferreira, M.J. Antibiotic Stewardship in Food-producing Animals: Challenges, Progress, and Opportunities. *Clin. Ther.* **2020**, *42*, 1649–1658. [[CrossRef](#)]
5. Stanton, I.C.; Bethel, A.; Leonard, A.F.; Gaze, W.H.; Garside, R. What is the research evidence for antibiotic resistance exposure and transmission to humans from the environment? A systematic map protocol. *Environ. Evid.* **2020**, *9*, 12. [[CrossRef](#)] [[PubMed](#)]
6. Wallinga, D. Don't ignore another disease threat. *Nature* **2020**, *586*, S64. [[CrossRef](#)]
7. Salmond, G.P.; Fineran, P.C. A century of the phage: Past, present and future. *Nat. Rev. Microbiol.* **2015**, *13*, 777–786. [[CrossRef](#)] [[PubMed](#)]
8. Keen, E.C. A century of phage research: Bacteriophages and the shaping of modern biology. *Bioessays* **2015**, *37*, 6–9. [[CrossRef](#)]
9. Sarhan, W.A.; Azzazy, H.M. Phage approved in food, why not as a therapeutic? *Expert. Rev. Anti-Infect. Ther.* **2015**, *13*, 91–101. [[CrossRef](#)] [[PubMed](#)]
10. Aleshkin, A.V.; Rubalskii, E.O.; Volozhantsev, N.V.; Verevkin, V.V.; Svetoch, E.A.; Kiseleva, I.A.; Bochkareva, S.S.; Borisova, O.Y.; Popova, A.V.; Bogun, A.G.; et al. A small-scale experiment of using phage-based probiotic dietary supplement for prevention of *E. coli* traveler's diarrhea. *Bacteriophage* **2015**, *5*, e1074329. [[CrossRef](#)]
11. Doss, J.; Culbertson, K.; Hahn, D.; Camacho, J.; Berekzi, N. A Review of Phage Therapy against Bacterial Pathogens of Aquatic and Terrestrial Organisms. *Viruses* **2017**, *9*, 50. [[CrossRef](#)]
12. Wójcik, E.A.; Stańczyk, M.; Wojtasik, A.; Kowalska, J.D.; Nowakowska, M.; Łukasiak, M.; Bartnicka, M.; Kazimierzczak, J.; Dastyk, J. Comprehensive Evaluation of the Safety and Efficacy of BAFASAL(R) Bacteriophage Preparation for the Reduction of Salmonella in the Food Chain. *Viruses* **2020**, *12*, 742. [[CrossRef](#)]
13. Sobel, J.; Hirshfeld, A.B.; Mctigue, K.; Burnett, C.L.; Altekruse, S.; Brenner, F.; Malcolm, G.; Mottice, S.L.; Swerdlow, C.R.N.L. The pandemic of Salmonella enteritidis phage type 4 reaches Utah: A complex investigation confirms the need for continuing rigorous control measures. *Epidemiol. Infect.* **2000**, *125*, 1–8. [[CrossRef](#)]
14. Caenepeel, C.; Tabib, N.S.S.; Vieira-Silva, S.; Vermeire, S. Review article: How the intestinal microbiota may reflect disease activity and influence therapeutic outcome in inflammatory bowel disease. *Aliment. Pharmacol. Ther.* **2020**, *52*, 1453–1468. [[CrossRef](#)] [[PubMed](#)]
15. Tang, W.H.W.; Bäckhed, F.; Landmesser, U.; Hazen, S.L. Intestinal Microbiota in Cardiovascular Health and Disease: JACC State-of-the-Art Review. *J. Am. Coll. Cardiol.* **2019**, *73*, 2089–2105. [[CrossRef](#)] [[PubMed](#)]
16. Miaoa, S.; Kaib, M.; Jiec, W.; Guangxiand, W.; Changliangd, Z.; Qic, L.; Xiaofenga, B.; Huia, W. A Review of the Brain-Gut-Microbiome Axis and the Potential Role of Microbiota in Alzheimer's Disease. *J. Alzheimer's Dis.* **2020**, *73*, 849–865.
17. Malkki, H. Parkinson disease: Could gut microbiota influence severity of Parkinson disease? *Nat. Rev. Neurol.* **2017**, *13*, 66–67. [[CrossRef](#)] [[PubMed](#)]
18. Simpson, C.A.; Mu, A.; Haslam, N.; Schwartz, O.S.; Simmons, J.G. Feeling down? A systematic review of the gut microbiota in anxiety/depression and irritable bowel syndrome. *J. Affect. Disord.* **2020**, *266*, 429–446. [[CrossRef](#)]
19. Divya Ganeshan, S.; Hosseinidoust, Z. Phage Therapy with a Focus on the Human Microbiota. *Antibiotics* **2019**, *8*, 131. [[CrossRef](#)]
20. Li, L.; Ning, Z.; Zhang, X.; Mayne, J.; Cheng, K.; Stintzi, A.; Figeys, D. RapidAIM: A culture- and metaproteomics-based Rapid Assay of Individual Microbiome responses to drugs. *Microbiome* **2020**, *8*, 33. [[CrossRef](#)]
21. Li, L.; Abou-Samra, E.; Ning, Z.; Zhang, X.; Mayne, J.; Wang, J.; Cheng, K.; Walker, K.; Stintzi, A.; Figeys, D. An in vitro model maintaining taxon-specific functional activities of the gut microbiome. *Nat. Commun.* **2019**, *10*, 4146. [[CrossRef](#)]
22. Mao, B.; Li, D.; Zhao, J.; Liu, X.; Gu, Z.; Chen, Y.Q.; Zhang, H.; Chen, W. Metagenomic insights into the effects of fructooligosaccharides (FOS) on the composition of fecal microbiota in mice. *J. Agric. Food Chem.* **2015**, *63*, 856–863. [[CrossRef](#)]
23. Gu, J.; Mao, B.; Cui, S.; Liu, X.; Zhang, H.; Zhao, J.; Chen, W. Metagenomic Insights into the Effects of Fructooligosaccharides (FOS) on the Composition of Luminal and Mucosal Microbiota in C57BL/6J Mice, Especially the Bifidobacterium Composition. *Nutrients* **2019**, *11*, 2431. [[CrossRef](#)]
24. Tandon, D.; Haque, M.M.; Gote, M.; Jain, M.; Bhaduri, A.; Dubey, A.K.; Mande, S.S. A prospective randomized, double-blind, placebo-controlled, dose-response relationship study to investigate efficacy of fructo-oligosaccharides (FOS) on human gut microflora. *Sci. Rep.* **2019**, *9*, 5473. [[CrossRef](#)]
25. Liu, F.; Li, P.; Chen, M.; Luo, Y.; Prabhakar, M.; Zheng, H.; He, Y.; Qi, Q.; Long, H.; Zhang, Y.; et al. Fructooligosaccharide (FOS) and Galactooligosaccharide (GOS) Increase Bifidobacterium but Reduce Butyrate Producing Bacteria with Adverse Glycemic Metabolism in healthy young population. *Sci. Rep.* **2017**, *7*, 11789. [[CrossRef](#)]
26. Sivieri, K.; Morales, M.L.V.; Saad, S.M.I.; Adorno, M.A.T.; Sakamoto, I.K.; Rossi, E.A. Prebiotic effect of fructooligosaccharide in the simulator of the human intestinal microbial ecosystem (SHIME(R) model). *J. Med.* **2014**, *17*, 894–901. [[CrossRef](#)]
27. Li, L.; Zhang, X.; Ning, Z.; Mayne, J.; Moore, J.I.; Butcher, J.; Chiang, C.; Mack, D.; Stintzi, A.; Figeys, D. Evaluating in Vitro Culture Medium of Gut Microbiome with Orthogonal Experimental Design and a Metaproteomics Approach. *J. Proteome Res.* **2018**, *17*, 154–163. [[CrossRef](#)]
28. Zhang, X.; Ning, Z.; Mayne, J.; Moore, J.I.; Li, J.; Butcher, J.; Deeke, S.A.; Chen, R.; Chiang, C.; Wen, M.; et al. MetaPro-IQ: A universal metaproteomic approach to studying human and mouse gut microbiota. *Microbiome* **2016**, *4*, 31. [[CrossRef](#)]
29. Cheng, K.; Ning, Z.; Zhang, X.; Li, L.; Liao, B.; Mayne, J.; Stintzi, A.; Figeys, D. MetaLab: An automated pipeline for metaproteomic data analysis. *Microbiome* **2017**, *5*, 157. [[CrossRef](#)]

30. Butcher, J.; Unger, S.; Li, J.; Bando, N.; Romain, G.; Francis, J.; Mottawea, W.; Mack, D.; Stintzi, A.; O'Connor, D.L. Independent of Birth Mode or Gestational Age, Very-Low-Birth-Weight Infants Fed Their Mothers' Milk Rapidly Develop Personalized Microbiotas Low in Bifidobacterium. *J. Nutr.* **2018**, *148*, 326–335. [[CrossRef](#)]
31. Mottawea, W.; Chiang, C.; Mühlbauer, M.; Starr, A.E.; Butcher, J.; Abujamel, T.; Deeke, S.A.; Brandel, A.; Zhou, H.; Shokralla, S.; et al. Altered intestinal microbiota-host mitochondria crosstalk in new onset Crohn's disease. *Nat. Commun.* **2016**, *7*, 13419. [[CrossRef](#)] [[PubMed](#)]
32. Li, M.; Lin, H.; Jing, Y.; Wang, J. Broad-host-range Salmonella bacteriophage STP4-a and its potential application evaluation in poultry industry. *Poult. Sci.* **2020**, *99*, 3643–3654. [[CrossRef](#)]
33. Ramirez, K.; Cazarez-Montoya, C.; Lopez-Moreno, H.S.; Campo, N.C. Bacteriophage cocktail for biocontrol of Escherichia coli O157:H7: Stability and potential allergenicity study. *PLoS ONE* **2018**, *13*, e0195023. [[CrossRef](#)]
34. Chijiwa, R.; Hosokawa, M.; Kogawa, M.; Nishikawa, Y.; Ide, K.; Sakanashi, C.; Takahashi, K.; Takeyama, H. Single-cell genomics of uncultured bacteria reveals dietary fiber responders in the mouse gut microbiota. *Microbiome* **2020**, *8*, 5. [[CrossRef](#)] [[PubMed](#)]